Treatment of Acid Mine Drainage (AMD) using industrial by-product: Sorption behavior of steel slag for metal-rich mine water

Mohd Syakirin Md Zahar[a], Faradiella Mohd Kusin[a,b,*], Khairul Nizam Mohamed[a,b], Noratiqah Masri[a]

[a]Department of Environmental Sciences, Faculty of Forestry and Environment, Universiti Putra Malaysia, 43400 UPM Serdang, Malaysia

[b]Institute of Tropical Forestry and Forest Products (INTROP), Universiti Putra Malaysia, 43400 UPM Serdang, Malaysia

*Corresponding author: faradiella@upm.edu.my

GRAPHICAL ABSTRACT

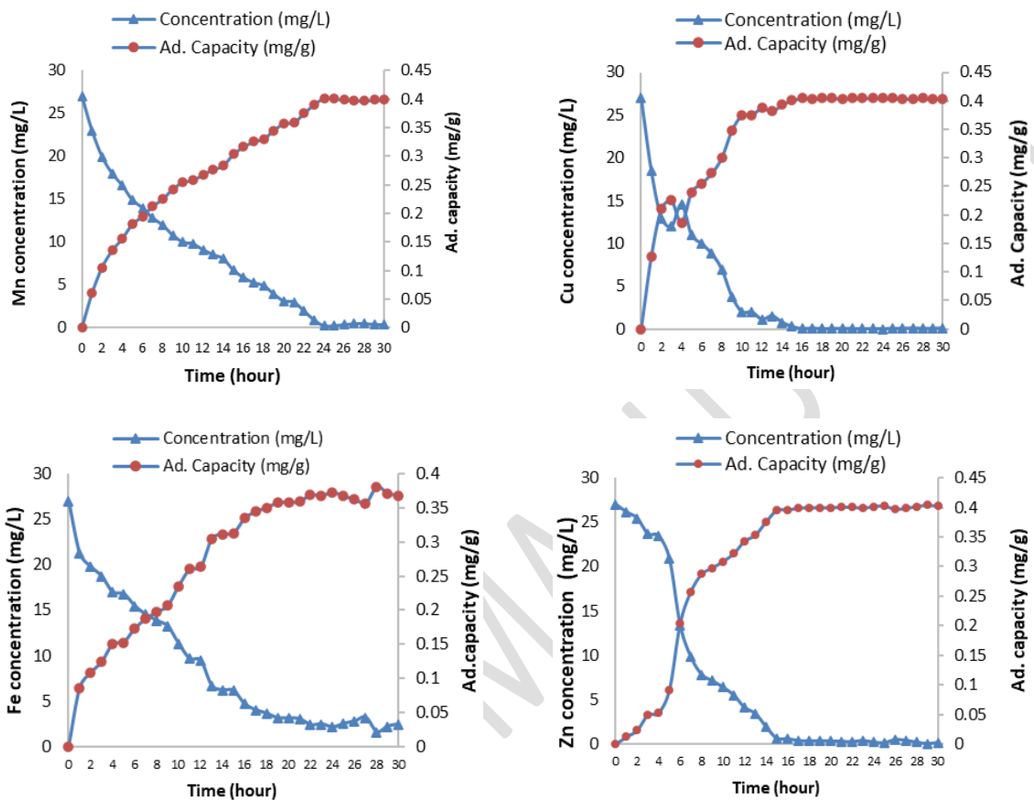

ABSTRACT

This study highlights the potential of steel slag, which is an industrial by-product of steel making industry as treatment media for metal-rich acid mine drainage (AMD). A series of batch adsorption studies has been done to demonstrate the effects of contact time, solution pH, initial concentration of metal, adsorbent dosage and size, and the effect of competing ions on the performance of steel slag. Results indicated that metal removal efficiencies were found to be >90% when pH of AMD has reached near-neutral state (6.8-7.5) that were mostly occurring within the first 14 hours of contact time. Optimum equilibrium time was found at 24 hours, i.e. 99-100% of metals were removed. An increased adsorption capacity with decreased removal efficiency was observed as initial metal concentration increased. In contrast, increasing adsorbent dosage leads to increased removal efficiency. Fe was not affected despite the presence of other metal ions (100% removal) compared to Mn (59.3% removal) in mixed AMD solution. Adsorption behavior of Fe, Cu, Zn and Mn fits appropriately with Langmuir isotherm model with adsorption capacity of 1.06, 1.03, 0.97 and 0.73 mg g^{-1}, respectively. The adsorption kinetics followed the pseudo-second-order kinetics and is supported by intra-particle diffusion process. Therefore, steel slag can be potentially used as an effective media for passive AMD remediation.

Keywords: Adsorption, Acid mine drainage, Heavy metal, Isotherm model, Industrial by-product, Steel slag

1. INTRODUCTION

Acid mine drainage (AMD) is a discharge of mining wastewater having characterized by its low pH and typically contains high concentration of sulfate and heavy metals. The extent of this contamination is highly variable, depending on the factors such as the nature of the ore body, geological strata, climate, and mining engineering constraints (Lee *et al.,* 2005; Carranza *et al.,* 2016; Madzin *et al.,* 2017). The metals were originated from dissolved sulfides and are held in solution due to their solubility in acidic waters. These heavy metals, which are not biodegradable, tend to cause various undesirable ecological impacts so as on human health (Diami *et al.,* 2016; Kusin *et al.,* 2017). In Malaysia, an example of AMD pollution has been reported due to a copper ex-mine in Mamut, Sabah (Jopony and Tongkul, 2009). The mine water was highly acidic (pH 3.0) with elevated concentration of some heavy metals in the mine effluent. Treatment of AMD may take various forms of physical, chemical and/or biological processes. Understanding the mechanism of pollutant removal from

AMD is essential to ensure that appropriate process may be incorporated in a treatment system. One of the potential applications for on-site remediation of metal-rich AMD is the use of steel slag leach beds, SSLB (Goetz and Riefler, 2014). This new innovative treatment technology has been a popular choice of AMD treatment in the US, for its promising performance for alkalinity generation thus neutralizing pH and precipitate metals.

Steel slag, which is a by-product of steel manufacturing industry, contains high concentrations of readily dissolvable alkalinity on its surface (e.g. $Ca(OH)_2$, Ca-(Fe)-silicates) (Ziemkiewicz, 1998; Huijgen *et al.,* 2005). It is primarily made of iron (Fe) and calcium (Ca) minerals (i.e. Fe derives from the raw minerals used to produce steel, while Ca derives from the use of fluxing agents such as lime during the steelmaking process (Motz and Geiseler, 2001). More specifically, steel slag contains Fe_2O_3 (42–84%), CaO (25–55%), SiO_2 (9–18%), Al_2O_3 (0–3%), and MnO (1–6%) (Haynes, 2015). It is an example of a solid waste material that can be used as a potential sorbent. The reported annual global steel slag production in Malaysia is fifty million tons and dumping it off is gradually becoming a major environmental issue (Yusuf *et al.,* 2014). Therefore, natural materials that are available in large quantities or certain waste products from industrial or agricultural processes may have potential as inexpensive sorbents. In this study, steel slag was used as an adsorbent for metal-rich AMD treatment potentially be applied as the media of treatment in SSLB for such cases.

Steel slags have shown promising performance in removing various heavy metals such as Zn, Cu, Pb Cd, Ni, and Cr, and phosphorus from aqueous solutions (Feng *et al.,* 2004; Jha *et al.,* 2004; Kim *et al.,* 2008; Liu *et al.,* 2009; Beh *et al.,* 2010; Song *et al.,* 2014; Barca *et al.,* 2012). Generally, the main constituents of the slag are iron oxides and calcium hydroxides. The function of iron oxides in the slag is to provide the adsorption sites for anions to be adsorbed (Fendorf *et al.,* 1997). Meanwhile, the calcium hydroxides contained in slag can increase the pH value of the surrounding system and lead to heavy metal cations precipitation (Zhang et al., 2008). Feng *et al.,* (2004) used steel slag and iron slag to remove Cu(II) and Pb(II) from synthetic wastewater. The adsorption of metals for the two slags fits well with the Langmuir isotherm. A study by Srivastava *et al.* (1997) uses steel slag to remove Pb and Cr in a batch and column experiment. The study revealed that reduction rate of Pb and Cr is fast and showed a potential to be used for real application. Steel slag had also been used to reduce carcinogenic Cr(VI) to less soluble and less toxic Cr(III) in contaminated groundwater or in synthetic solutions (Piatak *et al.,* 2015). Additionally, it has been found that nitrate removal from the aqueous solution was primarily related to Al, Fe, Si and Mn leached from the steel slag (Liyun et al., 2017).

The objective of this study are to determine the performance of steel slag in removing heavy metals from metal-rich AMD and to investigate the factors that affect the adsorption capacity of the steel slag. The adsorption isotherm and kinetics aspect were also investigated to provide a greater understanding of its performance for real on-site application.

2. MATERIALS AND METHODS

2.1 Preparation and characterization of adsorbent

Steel slag in this study was obtained from Mega Steel Sdn Bhd, one of the leading companies for steel production in Malaysia. The steel slag was washed with distilled water to remove any impurities and dried at 105°C for the period of 24 hours in an oven. The steel slag was then crushed and sieved into the sizes of 0.5 mm, 1 mm, 1.5 mm and 2 mm. The physical surface characteristics of steel slag (specific surface area and pore size) were determined using BET (Brunauer-Emmette-Teller) and BJH (Barrett-Joyner-Halenda) pore size distribution analysis. Scanning electron microscopy (SEM) along with Energy-Dispersive X-Ray (EDX) analyzer was used to obtain the morphological structure and also the elemental composition of the steel slag.

2.2 Preparation of synthetic AMD

Synthetic AMD was used in this study and was made up according to the composition of AMD at Mamut ex-copper mine, by taking the worst case scenario. This is because it was not possible to obtain the actual mine water from the site for the purpose of laboratory experiment. Selected metal compositions were chosen from those exceeding the recommended regulatory acceptable values and with acidic pH range. Stock solution of selected heavy metals (Mn, Cu, Fe and Zn) with concentration of 1000 mg L^{-1} each was prepared by dissolving an appropriate amount of $MnSO_4.H_2O$ (manganese (II) sulfate-1-hydrate), $CuSO_4.5H_2O$ (copper 2 sulfate-5hydrate), $FeSO_4.7H_2O$ (Iron (II) sulfate-7-hydrate) and $ZnSO_4.7H_2O$ (Zinc Sulfate-7-hydrate) with deionized water (Milipore Corp, USA). The stock solution was further diluted with deionized water to obtain desired concentration of heavy metals used in this study. 0.1 M H_2SO_4 was used to adjust the pH to the desired level (pH 2-4). All the chemicals and reagents used in this study were of analytical grade (Sigma-Aldrich, Bendosen).

2.3 Batch experiments

A series of batch experiments were conducted to assess the performance of heavy metals adsorption onto steel slag. The batch experiment was conducted for each of heavy metal in single component. An orbital shaker with agitation speed of 200 rpm was used throughout the experiment to ensure homogenous mixing. The experiments were carried out at maintained temperature between 24-25°C. During the experiment, all the solutions were tightly cap-covered to prevent any circumstances that might occur such as contamination and spillage. All solution samples were filtered using 0.45µm nylon membrane filter and kept at 4°C before analysis. The heavy metals concentration was analyzed using atomic absorption spectrophotometer (AAS). The samples from batch experiments were taken in duplicate to ensure the findings were precise and consistent. The batch tests were carried out for optimization of contact time and the adsorbent dosage while considering the effects of initial solution pH, initial metal concentration and adsorbent size. pH of aqueous solution is important for retention of ions onto adsorption surfaces while adsorbent size would have effect on surface area availability and porosity of media for particle adsorption.

2.3.1 Optimization of contact time

The optimum contact time was determined by mixing 2 g of adsorbent with the size of 0.5 mm into 30 mL of heavy metal solution at pH 3.0 within 24h. Following this, the effect of initial solution pH and metal concentration was also observed in relation to contact time. Using 0.1 M of H_2SO_4, the pH of heavy metal solutions were adjusted from 2.0 to 4.0 considering the pH range of AMD that were acidic. The effect of initial metal concentration was

determined by varying the concentration at 17, 27, 37, 47, 67 and 100 mg L^{-1} of heavy metal solution.

2.3.2 Optimization of adsorbent dosage

The optimum adsorbent dosage was determined by mixing 0.1, 0.2, 0.5, 1.0, 2.0 and 4.0 g of adsorbent into 30 mL of heavy metal solution at pH 3.0. This was followed by determination of the effect of adsorbent size on adsorption capacity. Various sizes of adsorbent of 0.5 mm, 1 mm, 1.5 mm and 2.0 mm were added into 30 mL heavy metal solution. In order to investigate the effect of competing ions on adsorption capacity, experiment was conducted using mixed solution containing the mixture of Mn, Fe, Cu and Zn.

2.4 Removal efficiency and adsorption capacity

Removal efficiency of adsorbent is calculated at time (qt) and also at equilibrium (qe). The removal efficiency is calculated as follows:
Removal percentage (%):

$$\frac{C_o - C_e}{C_o} \times 100 \quad (1)$$

$$\frac{C_o - C_t}{C_o} \times 100 \quad (2)$$

The amount of adsorbate adsorbed per unit mass of adsorbent, is calculated as:

$$\frac{C_o - C_t}{m} \times V \quad (3)$$

$$\frac{C_o - C_e}{m} \times V \quad (4)$$

Where C_o and C_e are the initial and final metal concentrations at equilibrium time (mg L^{-1}). C_t represents metal concentration of contact time (mg L^{-1}). V represents the volume of working solution (L) and m (g) is the mass of the adsorbent used.

2.5 Adsorption isotherms

Langmuir and Freundlich isotherm models were used in this study to analyze equilibrium data obtained from the removal of metal. The assumptions made in derivation of the Langmuir model are the adsorbed layer is made up of single layer of molecules with adsorption can only occur at a finite (fixed) number of definite localized sites, that are identical and equivalent, with no lateral interaction (Vijayaraghavan *et al.,* 2006). The Langmuir equation is given as follows:

$$\frac{C_e}{q_e} = \frac{1}{bq_m} + \frac{C_e}{q_m} \quad (5)$$

b and *qm* are Langmuir constants, which relate to the rate of adsorption (L mg^{-1}) and adsorption capacity (mg g^{-1}). Langmuir constant (*b* and *qm*) can be determined from the slope and intercept from linear graph of C_e/q_e versus C_e. The effect of Langmuir isotherm whether favorable or not can be determined by the following equation:

$$R_L = \frac{1}{1 + bC_0} \quad (6)$$

Where *b* is Langmuir constant and C_0 represents initial concentration of metal. The RL value indicates whether the isotherm is suitable for the adsorbent. When RL = 1, it indicates a linear relationship. The R_L > 1 value shows that the type of isotherm is not favorable, when 0 < R_L< 1, the isotherm is likely to be favorable and when R_L = 0 it shows an irreversible relationship. The Freundlich isotherm can be applied for non-ideal adsorption on heterogeneous surface and multilayer adsorption (Foo & Hameed 2010). The Freundlich equation is given as follows:

$$\log q_e = \log k_f + \frac{1}{n} \log C_e \quad (7)$$

k and *n* are Freundlich constant which can be obtained from the slope and intercept from linear graph of $\log q_e$ versus $\log C_e$.

2.6 Kinetics test

Lagergren's pseudo-first-order, pseudo-second-order and intra particle diffusion model were selected in this in this study to describe the kinetics of adsorption of heavy metals onto steel slag.

2.6.1 Pseudo first-order-kinetics

The Lagergren's pseudo-first-order equation can be expressed as (Ho 2004):

$$\log(q_e - q_t) = \log q_e - \frac{k_1}{2.303} t \quad (8)$$

Where q_e and q_t are adsorbate concentration at equilibrium and also at time (minute) while k_1 (min^{-1}) is the rate constant of this model. k_1 and q_e can be determined from the slope and also the intercept from the graph of log (q_e - q_t) versus t (minutes).

2.6.2 Pseudo second-order-kinetics

The pseudo-second-order equation can be expressed as (Ho and Mckay, 2000):

$$\frac{dq}{dt} = k_2 (q_e - q_t)^2 \quad (9)$$

This equation was integrated and can be rearranged to obtain a linear form:

$$\frac{t}{q_t} = \frac{1}{k_2 q^2{}_e} + \frac{t}{q_e} \quad (10)$$

Where k_2 (g mg^{-1} min) is the rate constant of this model. q_e and k_2 (g mg^{-1} min) can be determined from the slope and intercept of t/q_t versus t (minutes). Webber and Morris (1962) had proposed in intra particle diffusion model in 1962. The intra particle diffusion model can be written as:

$$q_t = k_i t^{1/2} + C \quad (11)$$

Where k_i is the intra particle diffusion rate constant (mg g^{-1} $min^{1/2}$). The intercept C, is proportional to the extent of the boundary layer thickness that is, the larger the intercept, the greater the boundary layer effect. The k_i can be determined from the slope of q_t (mg g^{-1}) versus $t^{1/2}$ ($min^{0.5}$) graph.

3. RESULTS AND DISCUSSION

3.1 Characteristics of steel slag

The surface and pore size characteristics, and the surface image of the steel slag have been presented in Zahar *et al.,* (2015), i.e. the surface area being 30.268 m^2 g^{-1}, pore volume of 0.028 mL g^{-1} and pore radius of 15.364 m^2 g^{-1}. Surface area of the steel slag is affected by size, shape, and porosity of particles, whereby smaller particle sizes tend to have larger surface area. The larger the surface area, the larger is the surface for adsorption to occur (Haynes, 2015). In addition, steel slag is also known to have high pH in the range of 11-12 (Xiong *et al.,* 2008; Zhou and Haynes, 2011).

EDX analysis has determined the major elements that are present before and after the adsorption of metals (Mn,

Fe, Cu and Zn) onto steel slag (Table 1). The EDX analysis revealed that the presence of Fe compound in the steel slag has helped as the surface catalyst for adsorption of metals especially for Fe. Notably the composition of steel slag is mainly composed of oxygen (33.32%) and calcium (22.09%), whilst appearance of Si (12.53%) and Fe (17.21%) were also significantly observed. The presence of initially high amount of aluminosilicate compound (aluminium, silicon, oxygen) in the presence of calcium oxide could facilitate in the provision of sufficient negatively charged sites for cation exchange reactions to take place with heavy metal present in aqueous solution (Aziz *et al.,* 2014; Muhammad *et al.,* 2017). Therefore, the presence of aluminosilicate is responsible for the removal of metal ions from the aqueous solution (Das *et al.,* 2007). As a result, the heavy metals that were initially non-exist (except for Fe) were found adsorbed onto the steel slag surfaces as shown in Table 1. Comparing between metals, Fe were found greatly adsorbed (40.98%) after the treatment compared to other metals. Apparently, this high adsorption of Fe might be attributable to the presence of Fe compound already exist in the steel slag that has helped as the surface catalyst (e.g. Fe oxides/hydroxides) for adsorption of this metal. In fact, materials that are rich in Fe amorphous and/or oxy-hydroxides can reduce the trace element bioavailability through sorption reactions, which consist of adsorption of metals on external surface, metal binding, fixation inside mineral particles and promotion of surface precipitation reactions (Violante *et al.,* 2008; Castaldi *et al.,* 2008). Furthermore, the processes of retention of metal/metalloid ions on particle surfaces are a combination of surface adsorption and surface precipitation (Apak, 2002; Bradl, 2004). The most important adsorbing surfaces are usually those on amorphous and crystalline Fe, Al, and Mn oxides and aluminosilicates (Haynes, 2015). Likewise, the effect of this surface catalyst has also helped in significant adsorption of Mn. Specific Mn adsorption onto the surfaces of the Fe oxides plus surface precipitation promoted by the high pH and residual alkalinity explains their metal adsorption capabilities (Zhou and Haynes, 2011).

Table 1 Elemental composition of steel slag before and after adsorption of metals

Elemental composition	**Initial weight (%)**	**Final weight (%)**			
		Mn*	Cu*	Fe*	Zn*
N	8.09	5.23	7.89	5.2	5.96
O	33.32	26.97	31.36	25.11	10.31
Mg	3.10	1.77	1.48	2.67	1.23
Al	3.66	1.22	3.11	2.81	1.65
Si	12.53	5.61	11.73	7.42	11.92
Ca	22.09	11.63	11.08	15.81	32.70
Fe	17.21	36.91	27.37	40.98	31.61
Mn	-	10.67	-	-	-
Cu	-	-	5.98	-	-
Zn	-	-	-	-	4.62
Total	100	100	100	100	100

*Treatment of respective metal adsorbed onto steel slag

3.2 Optimization of contact time

The effect of contact time was assessed to determine the optimum time for heavy metal adsorption onto steel slag. The time was set at 30 hours and reading was taken every 1 hour. Fig. 2 shows the effect of contact time and adsorption capacity of steel slag. General pattern shows that for the first 10 hours, the removal percentage indicates rapid increase (> 60%) and then slowly increases until it reached 24 hours. Higher removal percentage at the beginning of experiment is caused by the large surface area of steel slag that is available for the sorption of the metals (Yusuf *et al.,* 2013). Therefore, there are abundant free binding sites available that lead to the higher removal at early experiment (Aziz *et al.,* 2014). The removal percentage within 30 hours contact time can be seen in Fig. 1.

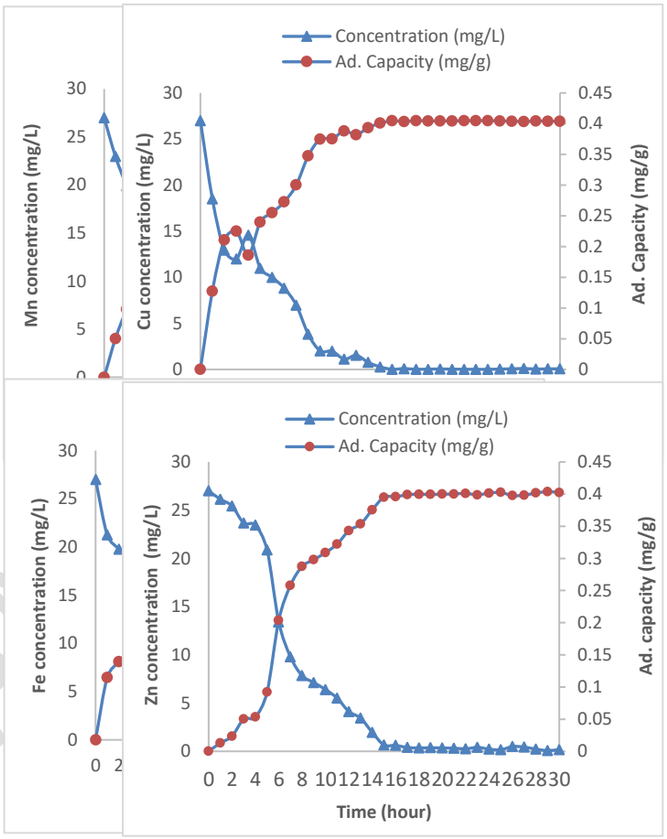

Generally, it was found that metal removal efficiencies were at >90% whenever pH of the solution has reached near-neutral state. The changes of solution pH from acidic to alkaline conditions were mostly found within the first 14 hours of treatment, whereby at this stage metals were rapidly removed (Fig. 2). Apparently, the removal of metals observed is attributed to not only the effect of contact time but also the changes in solution pH throughout the treatment. Comparing between metals, it is noticeable that removal of Mn was still low (i.e. about 60%) at near-neutral pH, whilst other metals have exhibited about 80-90% removals. Between 14-24 hours, removal of Mn was still rapidly occurring, whilst metals such as Cu and Zn have steadily achieved 99-100% removal. Notably, after 24 hours, the removals of all metals were almost constant and have reached 99-100% removal. Therefore, the equilibrium time was noted at 24 hours which is considered as optimum time enough to remove all these heavy metals from solution. The contact time was then set at 24 hours in all the following experiments

Fig. 1 Effect of contact time on adsorption of heavy metals onto steel slag (Initial concentration: 27 mg L^{-1}, dosage: 2 g, size: 0.5 mm, initial pH: 3)

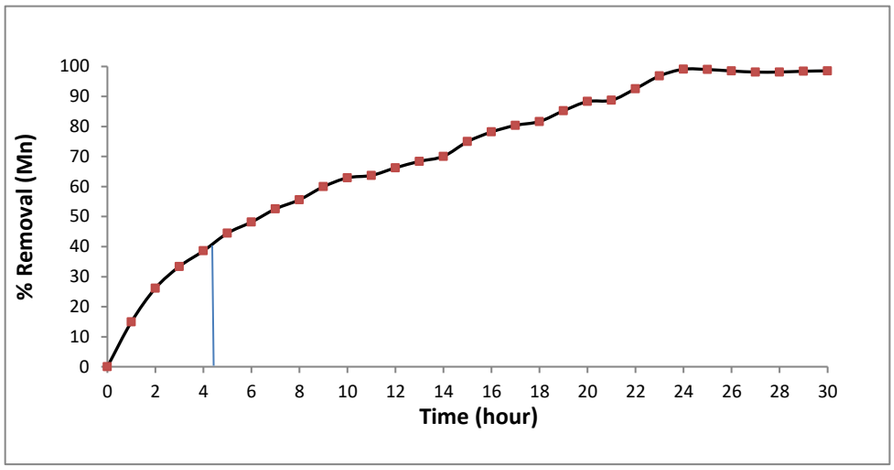

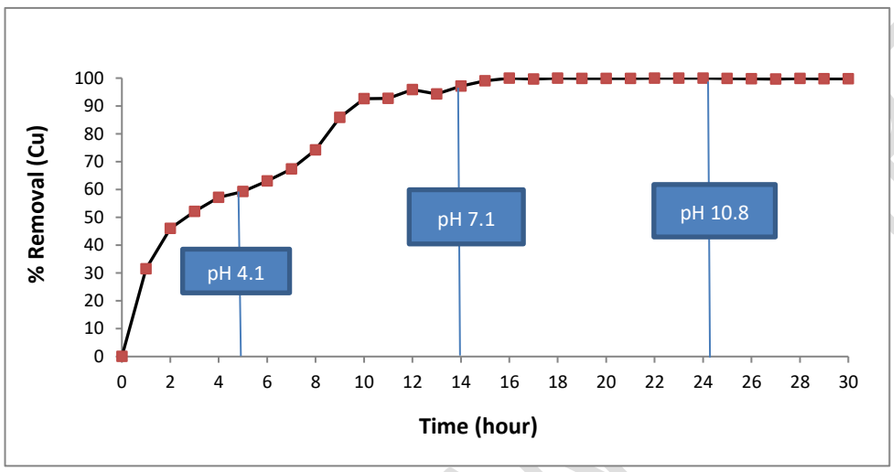

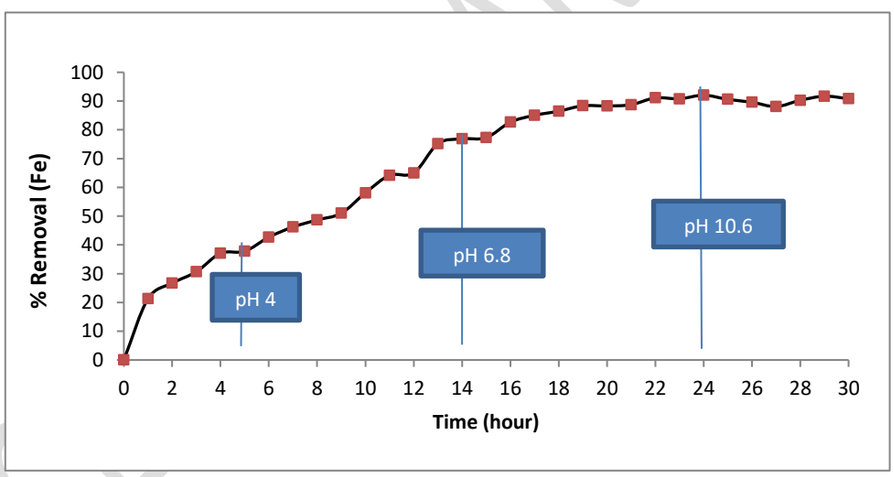

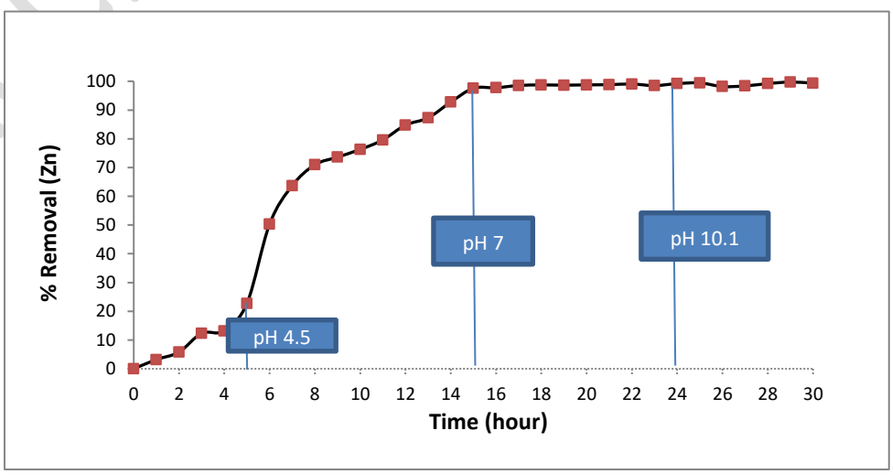

Fig. 2 Metal removal percentage as a function of time and changes in pH

3.3 *Effect of initial solution pH*

The pH of the metal ion solution is an important parameter for adsorption of heavy metal. In fact, the pH of the system is a key factor affecting retention of ions onto adsorption surfaces (Haynes, 2015). The adsorption of heavy metal greatly depends on the pH of aqueous solution (Omri and Benzina, 2012). This is because of hydrogen ion that competes with positively charged metal ion of the adsorbent (Lohani *et al.,* 2008). To examine the effect of pH on metal removal efficiency, the pH was varied from 2.0 to 4.0 as to reflect the acidic nature of the referred mine water. The percentage removal of heavy metal increases with the increase of pH. The lower removal at lower pH was also coupled with low adsorption rate, which is apparently due to higher concentration of hydrogen ion present in the reaction solutions, which can compete with metal ion for the adsorption sites. With an increase in pH, the competing effect of hydrogen ions decreased and the positively charged metal ion hook up with the free binding sites. Hence, the metal ion uptake is generally increased on the surfaces of the adsorbent with the increase in pH (Duan and Su, 2014; Muhammad *et al.,* 2015). Therefore, when the pH is reduced to an acidic condition, the hydrogen ions also increase thus increasing the competition between metal ions to be adsorbed on binding sites of adsorbent (Kour *et al.,* 2012).

3.4 *Effect of initial metal concentration*

The effect of different initial metal concentrations on removal efficiencies and adsorption capacity of steel slag was also evaluated. Fig. 3 shows the removal percentages and adsorption capacity of heavy metals onto steel slag. The heavy metal removals decrease when the initial concentration of heavy metal increases, while the adsorption capacity of heavy metal onto steel slag increases with the increase of initial heavy metal concentration. From the results, the highest initial concentration of 100 mg L^{-1} had the lowest removal percentage. Conversely, the adsorption capacity increases with the increase of initial concentration due to the driving force that is initiated by initial concentration to reduce the mass transfer resistance, resulting in higher adsorption capacity (Almasi *et al.,* 2012).

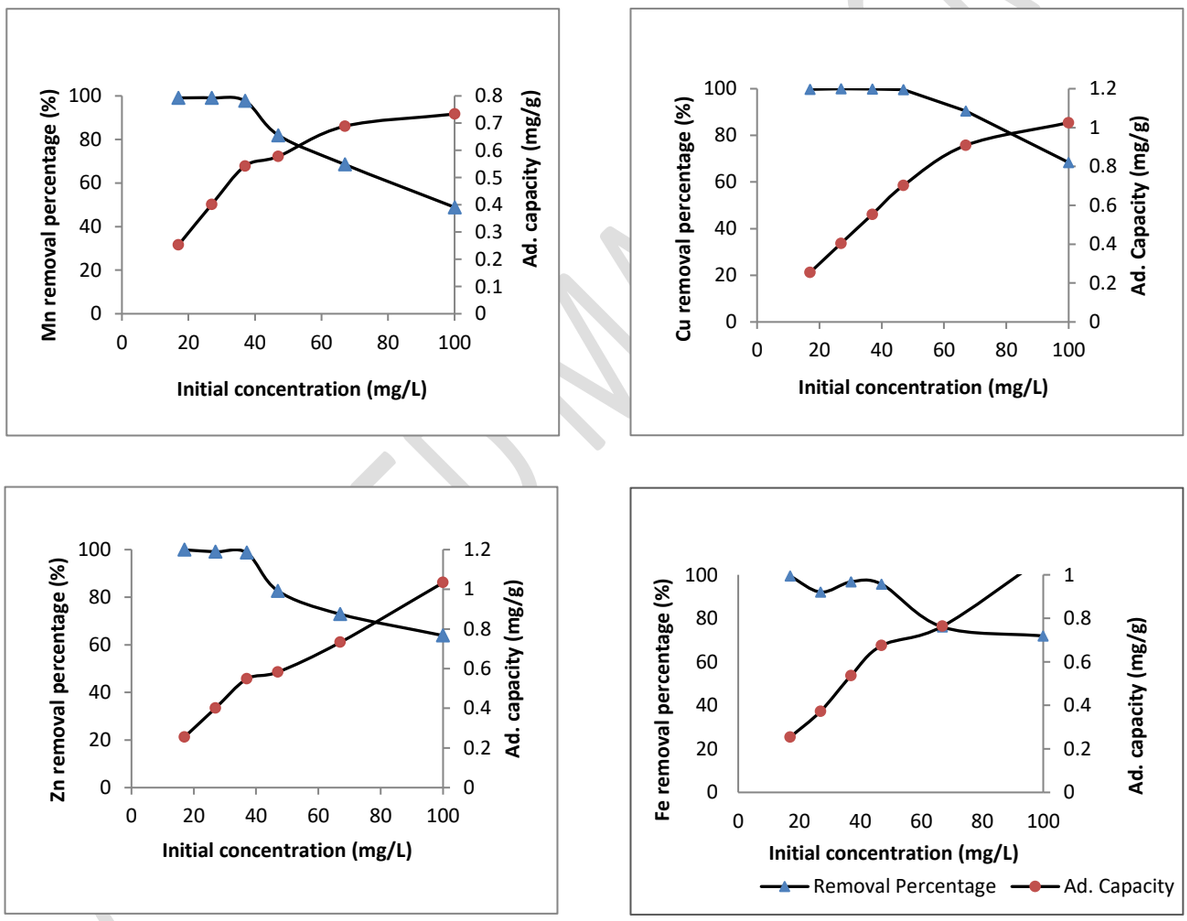

Fig.3 Effect of initial concentration (Contact time: 24 hours, size: 0.5 mm, dosage: 2g, Initial pH: 3)

3.5 *Optimization of adsorbent dosage*

Adsorbent dosage does have a great influence on the rate of adsorption. Fig. 4 shows the percentage removal of heavy metals using different adsorbent dosages ranging from 0.1 g until 4.0 g. There is a rapid removal when using adsorbent ranging from 0.1 until 2.0 g, i.e. removal percentage rapidly increased between 14.02% and 99.9%. Beyond 2.0 g of adsorbent, the percentage removal of heavy metal starts to become constant except for Fe. The initial rapid removal might be due to the increase in adsorbent surface and therefore results in more active site for metal adsorption (Kumar and Kirthika, 2009). However, at higher dosage, e.g. higher than 2.0 g of adsorbent, the removal percentage starts to become constant or no significant increase was observed due to saturation level has been attained during the adsorption process (Ragheb, 2013). In contrast, adsorption capacity was found decreased with the increase of adsorbent dosage. Several factors may contribute to this adsorbent dosage effect. The most important factor is that adsorption sites remain unsaturated during the adsorption of the adsorption reaction. This decrease in adsorption capacity with the increase in adsorbent dosage is mainly because of non-saturation of the adsorption sites during the adsorption process (Han *et al.,* 2006).

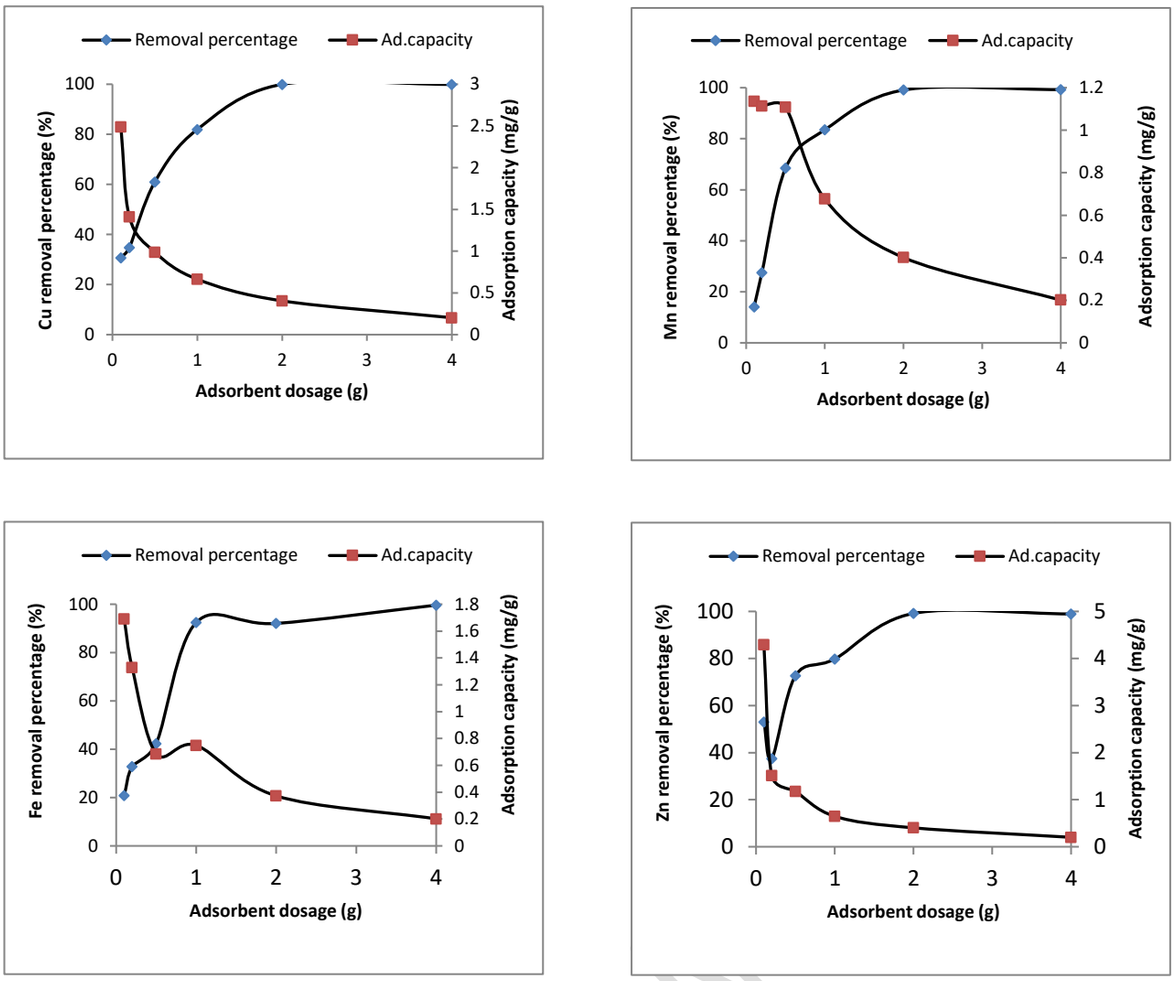

Fig.4 Effect of dosage (Initial concentration: 27 mg L^{-1}, contact time: 24 hours, size: 0.5 mm, initial pH: 3)

3.6 Effect of adsorbent size

Generally, small sizes have larger surface area. Removal percentages of greater than 90% for each metal element were observed in this experiment. For Mn and Zn, removals were at 99% at adsorbent size of 0.5-1.0 mm, however removals decreased to about 1-6% when adsorbent size increases between 1.5-2.0 mm. For Fe, removal was the highest at adsorbent size of 1.0 mm while for Cu the highest removal was observed at adsorbent size of 0.5 mm. Larger particle size has a longer diffusion path, while smaller particle has a shorter diffusion path, allowing adsorbate to penetrate quickly and deeply into the adsorbent particles, resulting in higher rate of adsorption (Yusuf *et al.,* 2013). Smaller particles sizes reduce internal diffusional and mass transfer limitation to penetration of the adsorbate inside the adsorbent. As noted earlier, surface area is affected by size, shape, and porosity of the particles. Particle size and porosity are important because treatment media need to be sufficiently permeable to allow water, solutes, and suspended material to flow through without clogging the treatment reactor. Therefore, it is wise to have a balance between finer particles to increase surface area (and thus increase adsorption) and coarser particles to increase porosity/hydraulic conductivity (Haynes, 2015).

3.7 Effect of competing ion

Because generally AMD contains multiple metal ions, thus it is important to know the performance of steel slag in dealing with competing ions for their removal from solution. The presence of multiple metal elements may result in competition between the metal ions to be adsorbed onto steel slag (Molahid *et al.,* 2018; Madzin *et al.,* 2020). Fig. 5 compares the removal percentage of metals from single and mixed element solution. It is clearly observed that Mn is highly affected with the presence of competing ions compared to the others metals, i.e. the lowest removal (59.3%) in mixed solution compared to single element. In contrast, Fe was not affected by the presence of competing ions, the fact that removal of Fe is even higher (100%) in mixed solution. This could be due to the presence of precipitates from other elements such as metal oxides or hydroxides that has served as the surface catalyst for more adsorption of Fe onto it. Cu was also not significantly affected by the presence of competing ions since removal percentages were almost the same in both single and mixed solution. On the other hand, removal of Zn was 18% lower in mixed solution compared to single element, suggesting that Zn is affected by the presence of other metal ions in the solution. Thus, adsorption/precipitation reactions are the main mechanisms by which adsorbent materials remove heavy metals from aqueous solution.

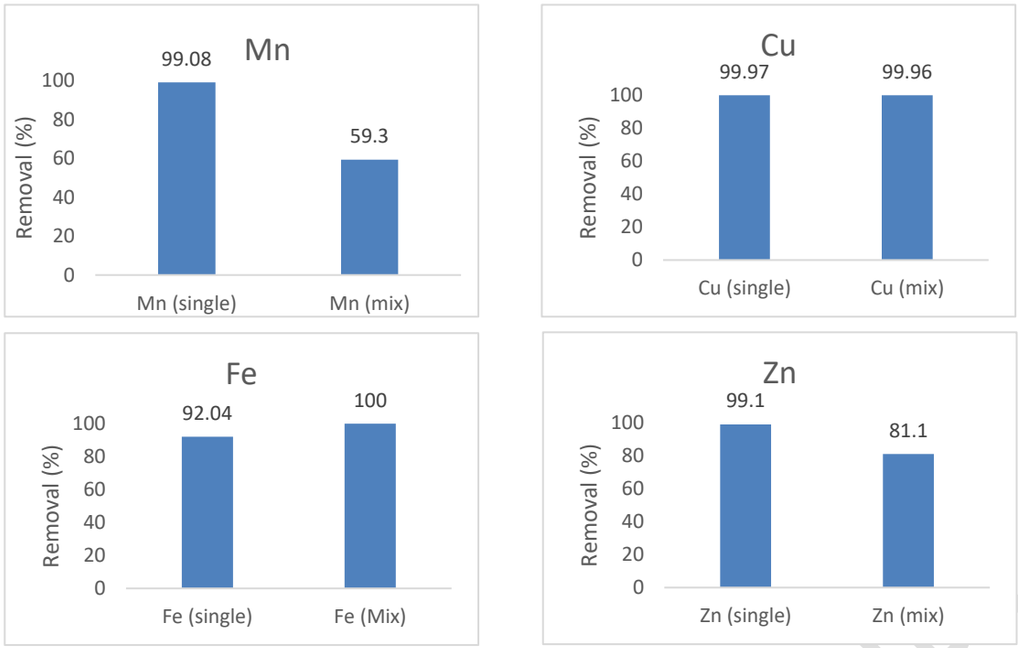

Fig. 5 Comparison of removal percentage for single and mixed solution

3.8 Adsorption isotherms

The data obtained were then used to determine the heavy metal adsorption isotherms. The equilibrium data were analyzed using Langmuir and Freundlich isotherm models, the two models that are generally used to describe adsorption isotherm of an adsorbent. In addition, adsorption isotherm can be described as a model that illustrates the distribution of the adsorbate species among adsorbent and liquid (Lu *et al.,* 2008). Adsorption data for heavy metal removal have been incorporated into this isotherm. Table 2 provides the Langmuir and Freundlich constants that are obtained from the slope and intercept of both plots. Langmuir model (R^2 of between 0.9523-0.9994) fits the data well compared to the Freundlich model (R^2 between 0.5836-0.9395) for all the metal elements. Therefore, this may be attributed to homogenous distribution of active sites on steel slag surfaces, based on the underlying assumption made in Langmuir equation (Foo and Hameed, 2010). Notably, this shows that Langmuir model better explains the adsorption of the heavy metals onto steel slag surfaces compared to Freundlich isotherm model. Additionally, the R_L values were also calculated which indicate whether the isotherm is suitable for the adsorbent according to the Langmuir model. It was noted that the values of R_L fell within the range $0<R_L<1$, suggesting that the adsorption of the heavy metals onto steel slag is favorable. Furthermore, the R_L values were also found approaching zero as with the increase in metal initial concentration, indicating the influence of initial concentration on the favorable adsorption mechanism.

Table 2 Isotherm constant values of Langmuir and Freundlich isotherm model

Mn		
Isotherm model	Parameters	Values
Langmuir isotherm	qm (mg g^{-1})	0.738
	b (L mg^{-1})	1.2027
	R^2	0.998
Freundlich isotherm	k	0.1592
	1/n	0.4399
	R^2	0.762
Cu		
Langmuir isotherm	qm (mg g^{-1})	1.0277
	b (L mg^{-1})	5.0653
	R^2	0.9994
Freundlich isotherm	k	0.1515
	1/n	0.7824
	R^2	0.5836
Fe		
Langmuir isotherm	qm (mg g^{-1})	1.0645
	b (L mg^{-1})	0.4757
	R^2	0.9523
Freundlich isotherm	k	0.2107
	1/n	0.4423
	R^2	0.7358
Zn		
Langmuir isotherm	qm (mg g^{-1})	0.9673
	b (L mg^{-1})	2.4186
	R^2	0.973
Freundlich isotherm	k	0.6547
	1/n	0.1832
	R^2	0.9395

3.9 Adsorption kinetics

The rate constant and other parameters for each kinetics model for metal adsorption onto steel slang are presented in Table 3. The theoretical q_e values obtained from the pseudo-first-order and pseudo-second-order kinetics were compared with experimental q_e values and there is large difference between pseudo-first-order compared to pseudo-second-order. The correlation coefficient, R^2 for pseudo-second-order shows better agreement compared to the correlation coefficient for pseudo-first-order which indicates that the adsorption of heavy metals onto steel slag fits well with the pseudo-second-order model. The pseudo-second-order model are based on the assumption that the rate limiting step may be chemical adsorption involving valence forces through sharing or the exchange of electrons between adsorbent and adsorbate (Ho and Mckay, 2000). One of the advantages of the pseudo-second-order equation for estimating q_e values is its small sensitivity to the influence of random experimental errors (Aly *et al.,* 2014).

The intra particle diffusion model is also presented in this study to assess the adsorption kinetics data in conjunction with pseudo-second-order model that is insufficient to predict diffusion mechanism (Akar *et al.,* 2008). Generally, the kinetic process of adsorption is always controlled by liquid film diffusion or intra particle diffusion in which one of the processes should be the rate limiting step (Qiu *et al.,* 2008). Intra particle diffusion plots may represent multi-linearity, which consider that two or three steps are involved in the adsorption process. In this form, the external surface adsorption or instantaneous adsorption occurs in the first step; the second step is the gradual adsorption step, where intra particle diffusion is controlled; and the third step where the solute moves slowly from larges pores to micro-pores causing a slow adsorption rate (Wu *et al.,* 2009). A plot of q_t vs $t^{1/2}$ would yield a straight line with a slope of k_i when the intra particle diffusion is a rate-limiting step (Qiu *et al.,* 2008). If the graph passes through origin, the intra particle diffusion process would not only be involved in adsorption process, but would be a rate limiting step (Aly *et al.,* 2014). From the analysis, the linear form obtained from a plot of q_t vs $t^{1/2}$ did not pass through origin thus indicating that the intra particle diffusion mechanism is not the sole rate determining step.

Table 3 Rate constant and parameter for each kinetic model

Element	Experimental q_e (mg g^{-1})	Pseudo 1st order			Pseudo 2nd order			Intraparticle diffusion model	
		k_1 (min^{-1})	q_e (mg g^{-1})	R^2	k_2 (g mg^{-1} min)	q_e (mg g^{-1})	R^2	k_i (mg g^{-1} min$^{1/2}$)	R^2
Mn	0.4013	0.0018	0.4455	0.8809	0.0032	0.5229	0.9655	0.0106	0.9954
Cu	0.4049	0.0067	1.2117	0.9071	0.0083	0.4846	0.9870	0.0094	0.8975
Fe	0.3728	0.0029	0.6031	0.9164	0.0027	0.5431	0.9259	0.0108	0.9766
Zn	0.4016	0.0055	1.3636	0.9154	0.0017	0.6853	0.9311	0.013	0.9521

4. CONCLUSIONS

This study has demonstrated the adsorption potential of steel slag which is an industrial by-product as a media for treatment of metal mine-impacted water. The results indicated that Fe was greatly removed among other metals present in the mine water due to high preferential adsorption of steel slag for Fe. General patterns showed rapid removal of metals during the first 10 hours of treatment and the equilibrium time was noted at 24 hours to remove all the metals from mine water (99-100% removal). The removal of metals is not only influenced by the effect of contact time but also the changes in solution pH and initial solution concentration. The percentage removal of heavy metal increases with the increase of pH, and is coupled with the increase of the adsorption capacity. Metal removal efficiencies were at >90% whenever pH of the solution has reached near-neutral state of about 7 at 14 hours contact time. Conversely, the heavy metal removals decreased when initial concentration of heavy metal increased.

It was found that higher adsorbent dosage leads to increased removal efficiency but tends to be constant after reaching equilibrium amount of 2.0 g. Increasing adsorbent dosage also leads to the decrease in adsorption capacity. The effect of adsorbent size varies between metal elements, whereby removals of Mn and Zn were at 99% at adsorbent size of 0.5-1.0 mm, but becomes lower at greater sizes. For Fe, removal was the highest at adsorbent size of 1.0 mm but for Cu the highest removal was observed at adsorbent size of 0.5 mm. Comparing between metals, Fe was not affected by the presence of competing ions, i.e. removal is 100% in mixed solution. In contrast, Mn is highly affected with the presence of competing ions as indicated by the lowest removal (59.3%) in mixed solution. According to the equilibrium studies, the selectivity sequence of the adsorption mechanism can be given as $Fe^{2+} > Zn^{2+} > Cu^{2+} > Mn^{2+}$, with good fits being obtained using Langmuir isotherm model compared to Freundlich isotherm model. The metals adsorption kinetics is reflected by the pseudo-second-order model and is supported by the intra particle diffusion process.

ACKNOWLEDGEMENTS

This work was supported by GP-IPS/9574900 and GP-IPM/9433300 research grants funded by the Universiti Putra Malaysia. The authors would like to express their gratitude to the laboratory staffs of Faculty of Environmental Studies, Universiti Putra Malaysia for technical assistance.

REFERENCES

Akar T., Ozscan A.S., Tunali S. and Ozscan A. (2008), Biosorption of a textile dye (Acid Blue 40) by cone biomass of *Thuja orientalis*: Estimation of equilbrium, thermodynamic and kinetic parameters, *Bioresources Technology* **99** (8), 3057-3065.

Almasi A., Omidi M., Khodadadian M., Khamutian R. and Gholivand M.B. (2012), Lead(II) and cadmium(II) removal from aqueous solution using processed walnut shell: kinetic and equilibrium study, *Toxicological & Environmental Chemistry* **94** (4), 660-671.

Aly Z., Graulet A., Scales N. and Hanley T. (2014), Removal of aluminium from aqueous solution using PAN-based adsorbent: characterization, kinetics, equilibrium and

thermodynamics studies, *Environmental Science and Pollution Research* **21** (5), 3972-3986.

Apak R. (2002), Adsorption of heavy metal ions on soil surfaces and similar substances. In: Hubbard AT (ed.) Encyclopedia of surface and colloid science, Marcel Dekker, New York.

Aziz A.S., Manaf L.A., Man H.C. and Kumar N.S. (2014), Kinetic modeling and isotherm studies for copper (II) adsorption onto palm oil boiler mill fly ash (POFA) as a natural low-cost adsorbent, *BioResources* **9** (1), 336-356.

Barca C., Gerente C., Meyer D., Chazarenc F. and Andres Y. (2012), Phosphate removal from synthetic and real wastewater using steel slags produced in Europe, *Water Research* **46** (7), 2376–2384.

Beh C.L., Chuah L., Choong T.S., Kamarudzaman M.Z. and Abdan K.A. (2010), Adsorption study of electric arc furnace slag for the removal of manganese from solution, *American Journal of Applied Sciences* **7** (4), 442-446.

Bradl H.B. (2004), Adsorption of heavy metal ions on soils and soil constituents, *Journal of Colloid and Interface Science* **277**, 1–18.

Carranza F., Romero R., Mazuelos A. and Iglesias N. (2016), Recovery of Zn from acid mine water and electric arc furnace dust in an integrated process, *Journal of Environmental Management* **165**, 175-183.

Castaldi P., Silvetti M., Santona L., Enzo S. and Melis P. (2008), XRD, FT-IR, and thermal analysis of bauxite ore-processing waste (red mud) exchanged with heavy metals, *Clay Mineral* **56**, 461–469.

Das B., Prakash S., Reddy P.S.and Misra V.N. (2007), An overview of utilization of slag and sludge from steel industries. *Resources, Conservation and Recycling* **50** (1), 40-57.

Diami S.M., Kusin F.M. and Madzin Z. (2016), Potential ecological and human health risks of mine-impacted sediments in Pahang, Malaysia, *Environmental Science and Pollution Research* **23** (20), 21086–2109.

Duan J. and Su B. (2014), Removal characteristics of Cd(II) from acidic aqueous solution by modified steel-making slag, *Chemical Engineering Journal* **246**, 160-167.

Fendorf S., Eick M.J., Grossl P. and Sparks D.L. (1997), Arsenate and Chromate Retention Mechanisms on Goethite, *Surface Structure. Environ. Sci. Technol.* **31**, 315–320.

Feng D., Van Deventer J.S.J. and Aldrich C. (2004), Removal of pollutants from acid mine wastewater using metallurgical by-product slags, *Separation and Purification Technology* **40**, 61–67.

Foo K.Y. and Hameed B.H. (2010), Insights into the modeling of adsorption isotherm systems, *Chemical Engineering Journal* **156** (1), 2-10.

Goetz E.R. and Riefler R.G. (2014), Performance of steel slag leach beds in acid mine drainage treatment, *Chemical Engineering Journal* **240**, 579–588.

Han R., Zou W., Zhang Z., Shi J. and Yang J. (2006), Removal of copper(II) and lead(II) from aqueous solution by manganese oxide coated sand: I. Characterization and kinetic study, *Journal of Hazardous Materials* **137** (1), 384-395.

Haynes R.J. (2015), Use of Industrial Wastes as Media in Constructed Wetlands and Filter Beds—Prospects for Removal of Phosphate and Metals from Wastewater Streams, *Critical Reviews in Environmental Science and Technology* **45** (10), 1041-1103.

Ho Y.S. (2004), Citation review of Lagergren's kinetic rate equation on adsorption reactions, *Scientometrics* **59** (1), 171-177.

Ho Y.S. and McKay G. (2000), The kinetics of sorption of divalent metal ions onto sphagnum moss peat, *Water Research* **34** (3), 735-742.

Huijgen W.J.J., Witkamp G.J. and Comans R.N.J. (2005), Mineral CO_2 sequestration by steel slag carbonation, *Environmental Science & Technology* **39**, 9676–9682.

Jha V.K., Kameshima Y., Nakajima A. and Okada K. (2004), Hazardous ions up-take behaviour of thermally activated steel-making slag, *Journal of Hazardous Materials* **B114**, 139–144.

Jopony M. and Tongkul F. (2009), Acid mine drainage at Mamut Copper Mine, Sabah, Malaysia. *Borneo Sciences* **3**, 83-94.

Kim D.H., Shin M.C., Choi H.D., Seo C.I. and Bae K. (2008), Removal mechanisms of copper using steel-making slag: adsorption and precipitation, *Desalination* **233**, 283–289.

Kour J., Homagai P.L., Pokhrel M.R. and Ghimire K.N. (2012), Adsorptive Separation of Metal Ions with Surface Modified Desmostachya bipinnata, *Nepal Journal of Science and Technology* **13** (1), 101-106.

Kumar P.S. and Kirthika K. (2009), Equilibrium and kinetics study of adsorption of nickel from aqueous solution onto bael tree leaf powder, *Journal of Engineering Science and Technology* **4** (4), 351-363.

Kusin F.M., Rahman M.S.A., Madzin Z., Jusop S., Mohamat-Yusuff F., Ariffin M. and Zahar M.S.M. (2017), The occurrence and potential ecological risk assessment of bauxite mine-impacted water and sediments in Kuantan, Pahang, Malaysia, *Environmental Science and Pollution Research* **24** (2), 1306-1321.

Lee J.S., Chon H.T. and Kim K.W. (2005), Human risk assessment of As, Cd, Cu and Zn in the abandoned metal mine site*, Environmental Geochemistry and Health* **27**(2), 185-191.

Lim H.S., Lee J.S., Chon H.T. and Sager M. (2007), Heavy metal contamination and health risk assessment in the vicinity of the abandoned Songcheon Au-Ag mine in Korea, *Journal of Geochemical Exploration* 98, 223-230.

Liu S.Y., Qu B., Gao J and Yang YJ. (2009), Adsorption behaviours of heavy metal ions by steel slag-an industrial solid waste, *Proceedings of the Third International ICBBE Conference on Bioinformatics and Biomedical Engineering*, Chengdu, China.

Liyun Y., Ping X., Maomao Y. and Hao B. (2017), The characteristics of steel slag and the effect of its application as a soil additive on the removal of nitrate from aqueous solution, *Environ Sci Pollut Res Int.* **24** (5), 4882-4893.

Lohani M.B., Singh A., Rupainwarb D.C. and Dharc D.N. (2008), Studies on efficiency of guava (Psidium guajava) bark as bioadsorbent for removal of Hg (II) from aqueous solutions, *Journal of Hazardous Materials* **159** (2-3), 626-629.

Lu C., Liu C. and Rao G.P. (2008), Comparisons of sorbent cost for the removal of Ni^{2+} from aqueous solution by carbon nanotubes and granular activated carbon, *Journal of Hazardous Materials* **151** (1), 239-246.

Madzin Z., Kusin F.M., Yusof F.M. and Muhammad S.N. (2017), Assessment of Water Quality Index and Heavy Metal Contamination in Active and Abandoned Iron Ore Mining Sites in Pahang, Malaysia, *MATEC Web of Conferences* **103**, 05010.

Madzin Z., Kusin F.M., Molahid V.L.M. and Hasan S.N.S. (2020), Passive remediation of mine impacted water using selected treatment media containing-bioreactor, *IOP Conference Series: Materials Science and Engineering* **736** (4), 042028.

Molahid V.L.M., Kusin F.M., Madzin Z. (2018) Role of multiple substrates (spent mushroom compost, ochre, steel slag and limestone) in passive remediation of metal-containing acid mine drainage. *Environmental Technology* doi.org/10.1080/09593330.2017.1422546

Motz H. and Geiseler J. (2001), Products of steel slags: an opportunity to save natural resources, *Waste Management* **21** (3), 285–293.

Muhammad S.N., Kusin F.M., Zahar M.S.M., Yusuff F.M. and Halimoon N. 2015 Passive treatment of acid mine drainage using mixed substrates: Batch experiments, *Procedia Environmental Sciences* **30**, 157-161.

Muhamad S.N., Kusin F.M. and Zahar M.S.M. (2017), Passive bioremediation technology incorporating lignocellulosic spent mushroom compost and limestone for metal- and sulfate-rich acid mine drainage, *Environmental Technology* **38** (16), 2003-2012.

Omri A. and Benzina M. (2012), Removal of manganese(II) ions from aqueous solutions by adsorption on activated carbon derived a new precursor: Ziziphus spina-christi seeds, *Alexandria Engineering Journal* **51** (4), 343-350.

Piatak N.M., Parsons M.B. and Seal R.R. (2015), Characteristics and environmental aspects of slag: a review, *Appl. Geochem.* **57**, 236–266.

Qiu H., Pan B.C., Zhang Q.J., Zhang W.M. and Zhang, Q.X. (2008), Critical reviews in adsorption kinetic models, *Journal of Zhejiang University SCIENCE A* **10** (5), 716-724.

Ragheb S.M. (2013), Phosphate removal from aqueous solution using slag and fly ash, *HBRC Journal* **9** (3), 270-275.

Song G., Wu Y., Chen X., Hou W. and Wang Q. (2014), Adsorption performance of heavy metal ions between EAF steel slag and common mineral adsorbents, *Desalination and Water Treatment* **52** (37-39), 7125-7132.

Srivastava S.K., Gupta V.K. and Mohan D. (1997), Removal of Lead and Chromium by Activated Slag—A Blast-Furnace Waste, *Journal of Environmental Engineering,* Vol. 123 (Issue 5).

Vijayaraghavan K., Padmesh T.V., Palanivelu K. and Velan M. (2006), Biosorption of nickel(II) ions onto Sargassum wightii: Application of two-parameter and three-parameter isotherm models, *Journal of Hazardous Materials* **133** (1-3), 304-308.

Violante A., Krishnamurti G.S.R. and Pigna M. (2008), Factor affecting the sorption–desorption of trace elements in soil environments. In: Violante A, Huang P, Gadd GM (eds.) *Biophysico-chemical Processes of Heavy Metals and Metalloids In Soil Environment*, Wiley and Sons, Inc., pp. 169–213.

Weber W.J. and Morris JC. (1962), Advances in water pollution research: removal of biologically resistant pollutant from wastewater by adsorption. *In: Proceedings of 1st International conference on water pollution symposium*, Pergamon Press, Oxford, Vol. 2, pp. 231-236.

Wu F.C., Tseng R.L. and Juang R.S. (2009), Initial behavior of intraparticle diffusion model used in the description of adsorption kinetics, *Chemical Engineering Journal* **153** (1-3), 1-8.

Xiong J., He Z., Mahmood Q., Liu D., Yang X. and Islam E. (2008), Phosphate removal from solution using steel slag through magnetic separation, *Journal of Hazardous Materials* 152, 211–215.

Yusuf M., Chuah L.A., Mohammed M.A. and Shitu A. (2013), Investigations of Nickel (II) removal from Aqueous Effluents using Electric Arc Furnace Slag, *Research Journal of Chemical Sciences* **3** (12), 29-37.

Yusuf M., Chuah L.A., Khan M.A. and Choong T.S. (2014), Adsorption of Nickel on Electric Arc Furnace Slag: Batch and Column Studies, *Separation Science and Technology* **49** (3), 388-397.

Zahar M.S.M., Kusin F.M. and Muhammad S.N. (2015), Adsorption of manganese in aqueous solution by steel slag, *Procedia Environmental Sciences* **30**, 145-150.

Ziemkiewicz P. (1998), Steel slag: applications for AMD control, *Proceedings of the 1998 Conference on Hazardous Waste Research*, pp. 44–59.

Zhang T.S., Liu F.T., Liu S.Q., Zhou Z.H. and Cheng X. (2008), Factors influencing the properties of a steel slag composite cement, *Advances in Cement Research,* Volume 20 (Issue 4), pp. 145-150.

Zhou Y.F. and Haynes R.J. (2011), A comparison of inorganic solid wastes as adsorbents of heavy metal cations in aqueous solution and their capacity for desorption and regeneration, *Water, Air and Soil Pollution* **218**, 457–470.